

Analytical Methods

Accepted Manuscript



This is an *Accepted Manuscript*, which has been through the Royal Society of Chemistry peer review process and has been accepted for publication.

Accepted Manuscripts are published online shortly after acceptance, before technical editing, formatting and proof reading. Using this free service, authors can make their results available to the community, in citable form, before we publish the edited article. We will replace this *Accepted Manuscript* with the edited and formatted *Advance Article* as soon as it is available.

You can find more information about *Accepted Manuscripts* in the [Information for Authors](#).

Please note that technical editing may introduce minor changes to the text and/or graphics, which may alter content. The journal's standard [Terms & Conditions](#) and the [Ethical guidelines](#) still apply. In no event shall the Royal Society of Chemistry be held responsible for any errors or omissions in this *Accepted Manuscript* or any consequences arising from the use of any information it contains.

Rapid and selective extraction of multiple sulfonamides in aqueous samples based on Fe₃O₄-chitosan molecularly imprinted polymers

Shili Qin,^a Liqiang Su^{*,b}, Peng Wang^{*,a} and Yuan Gao^b

Abstract: Highly selective magnetic molecularly imprinted polymers (MMIPs) for the adsorption of sulfonamides (SAs) were prepared by surface imprinted technology using active Fe₃O₄-chitosan (Fe₃O₄-CS) as the core and a mixture of sulfamethazine (SMZ) and sulfamethoxazole (SMX) as mixed template molecules. The optimum crosslinker types and contents were evaluated based on analysis of the adsorption parameters (Q , K_d and k) and regeneration of the MMIPs. The structure, morphology, magnetism, thermostability, adsorption and recognition properties of the MMIPs were characterized using Fourier transform infrared (FT-IR) spectroscopy, X-ray diffraction (XRD), scanning electron microscopy (SEM), vibrating sample magnetometer (VSM), thermogravimetric analysis (TGA) and re-binding experiments respectively. The results showed that the superparamagnetic particles with a homogeneous polymer film exhibited the maximum adsorption capacity ($Q_{(SMX)}=4.32 \text{ mg g}^{-1}$; $Q_{(SMZ)}=4.13 \text{ mg g}^{-1}$), good selective recognition of SAs ($k_{(SMX)}=3.52$; $k_{(SMZ)}=3.83$) and a fast adsorption rate ($t=9 \text{ min}$). Furthermore, molecularly imprinted polymers magnetic dispersive solid-phase extraction (MIPs-MDSPE) coupled with HPLC method was developed for the enrichment and determination of seven SAs in five different water samples, with recoveries and relative deviations (RSD) ranging from 85.02 to 102.98% and from 2.77 to 6.47%, respectively. SMX was detected in influent and effluent sewage samples, with concentrations of 112 and 64 ng L⁻¹, respectively.

Keywords: mixed templates molecularly imprinted polymers; Fe₃O₄-chitosan; sulfonamides; aqueous samples

1 Introduction:

Sulfonamides (SAs) have been among the most commonly used veterinary antibiotics for more than 70 years because of their low cost, low toxicity and broad spectrum of activity against common bacterial diseases^[1]. However the widespread and indiscriminate use of SAs contributes to a potential threat to human health and contaminates natural ecosystems through the food chain^[2-3]. It has been noted that up to 95% of an administered dose of human or veterinary drug can be unmetabolized and directly discharged into the environment. According to the statistics, more than 20,000 tons of SAs enter the environment worldwide every year^[4], creating concentrations that range from 0.01 to 19.2 μg L⁻¹ and 0.004 to 6.0 μg L⁻¹ in untreated and treated wastewater, respectively. Meanwhile a large amount of pathogen resistance has been caused by low levels of antibiotics^[5-7]. Therefore, the problem of environment sample contamination by SAs is great of concern. There is a growing interest related to their presence, persistence and fate in the environment^[8-13]. Due to the high sensitivity and broad linear range of HPLC-MS

1 and HPLC with other detectors, they are used as the most widely analytical methods for the evaluation of SAs and in 60% of the
2 total number of evaluations ^[14]. However compared with an efficient instrumental technology, sample pre-treatment always lags
3 behind, which often leads to many difficulties during pre-concentration and isolation.
4
5

6
7 In the analysis of aquatic environments, the pre-treatment of SAs represents a difficult task due to the high complexity of
8 the analysed matrices, low concentrations (ng L^{-1}) present and long extraction time when analysing a large volume of sample.
9 The specific selectivity of molecularly imprinted polymer (MIPs) resolves the first two problems. Molecularly imprinted
10 technology (MIT) is an efficient method for the preparation of tailor-made materials with a high affinity and selectivity towards a
11 given target molecules ^[15-18]. In recent years, MIPs have been widely used for extracting antibiotics, hormones, contraband
12 pharmaceuticals and dyes from different samples ^[19-22], such as food, feed, clinical samples and environmental samples ^[23-26].
13 There are some reports of SAs-MIPs, which used a kind of SAs as template molecule and methacrylic acid (MAA), 4-vinylpyridine
14 (4-Vpy), acrylamide (ACM) as conventional functional monomers ^[27-29]. However few of these studies were available for the
15 analysis of the complicated practical samples, because in the theory the imprinted sites of MIPs have the highest adsorption
16 capacity for the given target template molecule and exhibit low affinity or selectivity for the co-generic analytes of the template
17 molecule. To overcome this problem, mixed templates MIPs using more than one compound as templates have been prepared
18 ^[30-34], which not only express the specific recognition ability for the family analogues of template molecule but also remove the
19 interference compounds in complicated matrix. In our previous study ^[35] mixed templates MIPs of SAs were synthesized by bulk
20 polymerization and the reaction mechanism was investigated.
21
22

23 The last problem of the analysis of aquatic environments (long extraction time) has also been settled by magnetic dispersive
24 solid-phase extraction (MDSPE). It is developed because of its advantages, which includes easy management, sufficient contact
25 with the matrices and a relatively short sample preparation time compared with traditional SPE. The main superiority is that
26 MDSPE could isolate a small quantity of sorbent from a large amount of analytical sample in short time. In recent studies Fe_3O_4
27 and functionalized Fe_3O_4 have been widely used as a polymeric supporter because of their highly rigid matrix, magnetic
28 properties, and hydrophilic surfaces ^[36-40]. Ding et al. and Chen et al. have developed similar simple and fast SPE procedures to
29 determine the SAs in honey and poultry feed, respectively ^[41-42]. The former described that magnetic MIPs were synthesized by
30 bulk polymerization using sulfamerazine (SMR) as the template molecule; the latter used sulfamethazine (SMZ) as the template
31 molecule by surface imprinted polymerization supported by a $\text{Fe}_3\text{O}_4\text{-SiO}_2$ core. Compared with the traditional magnetic
32 supporters of Fe_3O_4 ^[43] and $\text{Fe}_3\text{O}_4\text{-SiO}_2$, $\text{Fe}_3\text{O}_4\text{-chitosan}$ ($\text{Fe}_3\text{O}_4\text{-CS}$) particles have relatively abundant active groups on their
33 surfaces, which ideally suit for imprinting various molecules and enhance imprinting effects.
34

35 Thus, the combination of MIPs and MDSPE (MIPs-MDSPE) as a new type pre-treatment method ideally provides a powerful
36
37
38
39
40
41
42
43
44
45
46
47
48
49
50
51
52
53
54
55
56
57
58
59
60

analytical tool with the characteristics of selectivity, simplicity and flexibility, which resolves almost all of these problems on the analysis of trace residues in environmental water samples. To the best of our knowledge there are few reports on practical application of MIPs-MDSPE, using mixed templates molecules and Fe_3O_4 -CS supporter, coupled with HPLC method for the trace detection for SAs in the environmental water samples.

In this work, the magnetic core-shell particles were synthesized by a surface imprinted polymerization method with Fe_3O_4 -CS as the core and MIPs as the shell. The schematic preparation process involved a couple of steps, including the functional modification of vinyl groups on the surface of Fe_3O_4 -CS core, MIPs layer polymerization, and finally extraction of the template molecules with the generation of specific recognition sites. The results of characterization and the adsorption properties of the Fe_3O_4 -CS@MIPs showed that the self-synthesized magnetic core-shell particles have a high affinity, selectivity, and easy separation behaviour. Finally an efficient and highly selective MIPs-MDSPE coupled with HPLC method was established for the quantitative determination of seven SAs residues presented in aquatic samples at different levels.

2 Experimental

2.1 Chemicals and materials

Sulfathiazole (STZ), sulfadiazine (SDZ), sulfadimethoxine (SDM), sulfisoxazole (SIX), SMR, SMZ, SMX, cefradine (CED), cefotamix (CTX), trimethoprim (TMP), 3-methacryloyloxypropyltrimethoxy-silane (MPS) and formic acid (FAC) were purchased from Sigma-Aldrich (Steinheim, Germany). Chitosan with a molecule weight of $600,000 \text{ g mol}^{-1}$ and a degree of deacetylation of 87% was purchased from the Yuhuan Jingke Biology Co., Ltd. (Zhejiang, China). Ferric chloride hexahydrate ($\text{FeCl}_3 \cdot 6\text{H}_2\text{O}$) and ferrous chloride tetrahydrate ($\text{FeCl}_2 \cdot 4\text{H}_2\text{O}$) were purchased from the Tianjin Bodi-Chemical Co., Ltd. (Tianjin, China). 2-vinyl pyridine (2-Vpy), ethylene glycol dimethacrylate (EDMA), divinyl-benzene (DVB) and trimethylolpropane trimethacrylate (TRIM) were purchased from Acros Organics (Beel, Belgium). Methanol, ethanol, acetonitrile (ACN), methylbenzene, acetic acid (HAc), azo-bis-isobutyronitrile (AIBN), ammonium hydroxide ($\text{NH}_3 \cdot \text{H}_2\text{O}$) and other reagents were purchased from Kermel (Tianjin, China). Ultra-pure water was obtained from a Milli-Q water purification system (Millipore, Bedford, MA, USA). Standard stock solutions of SAs (1 mg mL^{-1}) were prepared in methanol and diluted to the required concentration with ultra-pure water. All solutions were stored at $4 \text{ }^\circ\text{C}$.

2.2 Preparation of vinyl-modified Fe_3O_4 -CS

The preparation of vinyl-modified Fe_3O_4 -CS was a two step synthetic procedure. (1) Fe_3O_4 -CS particles were prepared according to the previous report^[44]. Typically a solution was made by mixing 44 mL of ferric salt aqueous solution (0.7 g $\text{FeCl}_3 \cdot 6\text{H}_2\text{O}$ and 0.3 g $\text{FeCl}_2 \cdot 4\text{H}_2\text{O}$) and 200 mL of 0.25% (v/v) HAc aqueous solution of 3.0 mg mL^{-1} chitosan under a nitrogen atmosphere. After being stirred for 1 h at $40 \text{ }^\circ\text{C}$, 20 mL of $\text{NH}_3 \cdot \text{H}_2\text{O}$ was added drop by drop into the mixed solution under

1 vigorous stirring in 0.5 h. Fe₃O₄-CS particles were collected using a magnet and washed consecutively with 0.25% (v/v) HAc
2 aqueous solution, deionized water, acetone and methylbenzene until the Fe₃O₄-CS particles were evenly dispersed in 100mL of
3 methylbenzene solution. (2) Silane coupling agent (MPS) was used to graft vinyl groups on the surfaces of the magnetic core.
4
5 20 mL of the above-mentioned suspending solution of Fe₃O₄-CS particles was diluted by 80 mL of methylbenzene and dispersed
6 evenly by ultrasound. The mixture, to which 6 mL of MPS was added drop-wise, was stirred vigorously. The mixture was reacted
7 for 24 h at 30 °C under continuous stirring and a nitrogen atmosphere. The resultant product was collected by an external
8 magnetic field, rinsed with methanol and dried under a vacuum.
9

15 **2.3 Preparation of Fe₃O₄-CS@MIPs**

16
17
18 The MIPs shell was prepared by following a non-covalent imprinting approach. 1 mmol of SMZ and 1 mmol of SMX as mixed
19 templates and 4 mmol of 2-Vpy as functional monomer were mixed in 60 mL of ACN/toluene (3/1, v/v). The mixture was
20 pre-polymerized for 8 h at room temperature. Then, 100 mg of vinyl-modified Fe₃O₄-CS particles, 0.36 mmol of AIBN and
21 cross-linker (EDMA, DVB and TRIM) were added to the pre-polymerized mixture followed by ultrasonication for 10 min. The
22 mixture was heated to reflux at 60 °C for 24 h under mechanical stirring and a nitrogen atmosphere. According to the previous
23 work, which used EDMA as cross-linker and the reactant molar ratio of mixed templates, functional monomer and cross-linker
24 was 1:1:4:20, and the reactant molar ratio in this experiment was in the range from 1:1:4:14 to 1:1:4:24. Upon completion of the
25 synthesis, Fe₃O₄-CS@MIPs were washed with methanol/formic acid (90/10, v/v) for 12 h and pure methanol for 24 h in turn
26 using a Soxhlet extraction method. Meanwhile, in order to completely remove templates from the polymer, the eluent of the
27 Soxhlet extractor was detected by HPLC until the templates were not detected. Finally Fe₃O₄-CS@MIPs were dried at 60 °C under
28 vacuum. Fe₃O₄-CS non-imprinted polymers (Fe₃O₄-CS@NIPs) were prepared analogously in the absence of template molecules.
29

30 **2.4 Characterization of Fe₃O₄-CS@MIPs**

31
32
33
34
35
36
37
38
39
40
41
42
43
44
45
46
47
48
49
50
51
52
53
54
55
56
57
58
59
60
Fourier transform infrared spectra (FT-IR, 4000-400 cm⁻¹) were recorded on an Avatar 360 apparatus (Nicolet). X-ray
diffraction (XRD, 20-80 °) analysis was measured on a D8-Focus X-ray diffractometer (Bruker Optics). Scanning electron
microscopy (SEM) images were obtained on an S-4300 (Hitachi). Magnetic properties were measured on a Lakeshore 7300VSM
(Lakeshore Cryotronic, 300 K). Thermogravimetric analysis (TGA) was performed using a DiamondTG/DTA instrument
(PerkinElmer) under a nitrogen atmosphere.

51 **2.5 HPLC analysis**

52
53
54
55
56
57
58
59
60
Chromatographic analysis was performed on an Agilent1100 HPLC system (Palo Alto, CA, USA) equipped with a diode array
detector (DAD) using 0.5% v/v formic acid in water (A) and methanol(B) as the eluents. The gradient program was conducted as
follows: 0-5min 90-80% (A); 5-12 min 80-60% (A); and 12-20 min 60-35% (A). Finally (A) was recycled to 90% for 2.0 min and

1 equilibrated for 5.0 min with a flow rate of 1 mL min⁻¹. A Diamosil C18 (5- μ m-diameter particles, 4.6 mm \times 250 mm) analytical
2 column was used for the separation of the analytes. The LC column temperature was set at 30 °C. The injection loop volume for
3 LC experiments was 10 μ L or 50 μ L. The DAD system was set to 270 nm according to the maximum adsorption wavelengths of
4 SAs.
5
6
7
8

9 **2.6 Batch mode binding experiments**

10
11 There were three binding experiments for evaluating the adsorption properties of Fe₃O₄-CS@MIPs and Fe₃O₄-CS@NIPs: an
12 isothermal adsorption experiment, a kinetic adsorption experiment and a specific recognition adsorption experiment.
13

14 In the isothermal adsorption experiment, 10 mg of Fe₃O₄-CS@MIPs or Fe₃O₄-CS@NIPs were added to 10mL of a mixed
15 aqueous solution of SMZ and SMX with various concentrations ranging from 10 to 350 μ g mL⁻¹. The mixture was incubated for 2h
16 at room temperature after ultrasonic vibration. The supernatants and polymers were isolated by an external magnetic field, and
17 then the concentrations of SAs before and after adsorption in the solvent phase were measured by HPLC.
18
19

20 In the kinetic adsorption experiment, 10 mg of Fe₃O₄-CS@MIPs or Fe₃O₄-CS@NIPs were added to 10 mL of a 300 μ g mL⁻¹
21 mixed solution of SMZ and SMX, and then it was incubated and measured by HPLC at set intervals from 0 min to 30 min.
22

23 The procedure of the specific recognition adsorption experiment was similar to that of the isothermal adsorption
24 experiment. A mixed aqueous solution (240 μ g mL⁻¹) was prepared in blank wastewater containing seven SAs and common
25 antibiotics of CED, CTX and TMP.
26
27

28 The adsorption capacity (Q_e), the partition coefficients (K_d), the relative selectivity coefficients (k) and the selectivity
29 coefficients (k') values were calculated according to the following equations
30
31

$$32 Q_{max} = (C_i - C_e)V/m$$

$$33 K_d = Q_e/C_f$$

$$34 k = K_{MMIPs}/K_{MNIPs}$$

$$35 k' = k_{SMZ}/k_i$$

36 where C_i and C_e are the initial and equilibrium adsorption concentrations of the analytes in the aqueous solution, respectively, V
37 and m are the volume of the solution and the mass of the polymer, respectively, and Q_{max} is the maximum adsorption capacity.
38
39

40 **2.7 Method validation and practical sample application**

41 The method validation parameters were estimated by measuring the linearity, limits of detection (LOD) and precision. A
42 series of mixed working standard solutions of the analytes were diluted with ultrapure water to seven concentrations ranging
43 from 10 to 2000 ng mL⁻¹. Spiked recoveries and the precision were determined by evaluating seven SAs spiked six consecutive
44 times at concentrations of 20, 200 and 1000 ng mL⁻¹ in 500 mL blank water samples. Additionally, the LOD and enrichment factor
45
46
47
48
49
50
51
52
53
54
55
56
57
58
59
60

(EF) were calculated based on a signal-to-noise ratio of 3 ($S/N = 3$) of the HPLC profile and the ratio of the SAs concentration of pre-extraction and post-extraction, respectively.

Water samples were collected from five sites in Qiqihar including drinking water, Laodong Lake water, Nenjiang River water, and influent as well as effluent wastewater of Qiqihar sewage treatment in June of 2014. The pretreatment of the freshly collected water samples was performed immediately by filtering them through a 0.45- μm filter (Navigator, Lab Instrument) to remove suspended particles and adjusting the pH to 4.0 with buffer before DSPE.

50 mg of $\text{Fe}_3\text{O}_4\text{-CS@MIPs}$ was put into 500 mL of water sample, and the mixture was stirred homogeneously and incubated for 20 min. Then, the supernatants and polymers were isolated by an external magnetic field. Subsequently, the polymer-adsorbed SAs were transferred into a 3mL SPE cartridge. Finally, the SAs were desorbed with 5×1.0 mL of methanol. The eluents were combined, dried under N_2 and the residues were re-dissolved with 1 mL of the mobile phase for HPLC analysis

3 Results and discussion

3.1 Preparation of $\text{Fe}_3\text{O}_4\text{-CS@MIPs}$

The synthesis of $\text{Fe}_3\text{O}_4\text{-CS@MIPs}$ by a multistep protocol was described in Fig.1: (1) preparation of the vinyl-modified $\text{Fe}_3\text{O}_4\text{-CS}$ magnetic cores included the one-step synthesis of hybrid materials of $\text{Fe}_3\text{O}_4\text{-CS}$ and grafting vinyl groups on the surfaces of $\text{Fe}_3\text{O}_4\text{-CS}$; (2) $\text{Fe}_3\text{O}_4\text{-CS@MIPs}$ was prepared with the pre-polymeric mixture (template molecules and functional monomers), crosslinker and initiator by radical polymerization on the surfaces of the magnetic cores. And then the resulting particles with recognition cavities were obtained by eluting the template molecules.

In this work $\text{Fe}_3\text{O}_4\text{-CS}$ cores have been synthesized by a one-step co-precipitation method in which amino and hydroxyl groups of CS were chelated with Fe ions. Meanwhile, there were many residual amino and hydroxyl groups on the surfaces of the $\text{Fe}_3\text{O}_4\text{-CS}$ particles, which could be chemically modified. Compared with supports such as SiO_2 [29, 45], $\text{Fe}_3\text{O}_4\text{-SiO}_2$ [46], carbon nanotubes [47] and $\text{Fe}_3\text{O}_4\text{-wollastonite}$ [48] used in previous studies, $\text{Fe}_3\text{O}_4\text{-CS}$ particles distinctly improve grafting efficiency. Subsequently, the surface vinyl groups were grafted by the hydroxyl groups of $\text{Fe}_3\text{O}_4\text{-CS}$ further reacting with the MPS.

Afterwards the shell of MIPs was co-polymerized on the surface of vinyl group-functionalized $\text{Fe}_3\text{O}_4\text{-CS}$. To make the MIPs display a high affinity, selectivity and appreciable binding capacities for the analytes, the factors including the monomer types, crosslinker types and the molar ratio of the reactants should be taken into account. According to the previous work [35, 49], the templates of SMZ and SMX with both hydrogen-bond donors ($-\text{NH}_2$ and $-\text{NH}-$ groups) and weak acidities can form non-covalent interactions with the 2-Vpy monomer, which has both a hydrogen-bond acceptor (N atom of pyridine) and alkalinity. The molar ratio of the mixture of templates and monomer was chosen to be 1:1:4. In this work, the effects of the crosslinker type and molar reactant ratio on Q_{max} , K_d and k were further investigated. The results in Table 1 showed that MIPs prepared with the

1 trifunctional crosslinker (TRIM) provided a higher adsorption capacity ($Q_{(SMX)}=4.32 \text{ mg g}^{-1}$; $Q_{(SMZ)}=4.13 \text{ mg g}^{-1}$) and a better
2 flexibility and selectivity balance than those synthesized with EDMA or DVB within the MIP1-MIP3 polymer series. This result was
3
4 flexibility and selectivity balance than those synthesized with EDMA or DVB within the MIP1-MIP3 polymer series. This result was
5 obtained because the high degree of cross-linking enabled the recognition cavities to maintain three-dimensional structures
6 complementary in both shape and chemical functionality after the removal of the template molecules. Meanwhile, the
7 adsorption capacity of the MIPs with DVB was higher than that with EDMA, which was the benefit from additional hydrophobic
8 interactions and the aromatic stacking of the former.

9
10
11
12
13 Then the amount of crosslinker was discussed and evaluated in the polymers MIP3 and MIP4-MIP6 because that the
14 regeneration parameter of the resulting particles was important for subsequent application in the water samples. The adsorption
15 capacities and loss factors (LF) ranged from 1.62 to 4.32 mg g^{-1} and from 4.17 to 13.26%, respectively. It was obvious that MIP3
16 has a higher capacity and better stability than the other samples after 6 binding/regeneration cycles. This result indicated that
17 when the amount of crosslinker was reduced, the synthetic polymers were too soft to form stable affinity sites; however, an
18 extremely large amount of crosslinker could lead to a higher degree of crosslinking thus masking the recognition cavities. After
19 optimization, MIP3 was used in further experiments.

26 **3.2 Characterization of $\text{Fe}_3\text{O}_4\text{-CS@MIPs}$**

27
28
29 To realize the structures of the polymers from the main functional groups, Fig.2 compared FT-IR spectra of $\text{Fe}_3\text{O}_4\text{-CS}$ (a)
30 vinyl-modified $\text{Fe}_3\text{O}_4\text{-CS}$ (b) and $\text{Fe}_3\text{O}_4\text{-CS@MIPs}$ (c). The peak at approximately 574 cm^{-1} was attributed to Fe-O bond stretching
31 in $\text{Fe}_3\text{O}_4\text{-CS}$, vinyl-modified $\text{Fe}_3\text{O}_4\text{-CS}$ and $\text{Fe}_3\text{O}_4\text{-CS@MIPs}$. In the spectrum of $\text{Fe}_3\text{O}_4\text{-CS}$, compared with the standard spectrum of
32 CS, the 1589 cm^{-1} peak due to N-H bending vibrations shifted to 1556 cm^{-1} , and a peak at 1633 cm^{-1} appeared, indicating that CS
33 reacted with glutaraldehyde to form a Schiff base. Meanwhile in vinyl-modified $\text{Fe}_3\text{O}_4\text{-CS}$ spectrum, a new weak peak at 1706
34 cm^{-1} from the C=O group vibration verified that MPS successfully modified the magnetic particles. Moreover, the stronger
35 absorption peaks at 1731 cm^{-1} , 1159 cm^{-1} and 1072 cm^{-1} in the $\text{Fe}_3\text{O}_4\text{-CS@MIPs}$ spectrum were assigned to the C=O stretching
36 vibration and C-O symmetric and asymmetric stretching vibrations of the ester group. In the three spectrums, the absorption
37 bands at 3428 cm^{-1} , 2925 cm^{-1} and 2854 cm^{-1} were attributed to the stretching vibrations of O-H and C-H, respectively. These
38 characteristic absorption bands confirmed that the MIPs coatings were co-polymerized on the surface of $\text{Fe}_3\text{O}_4\text{-CS}$.

39
40
41
42
43
44
45
46
47
48
49 The XRD patterns of Fe_3O_4 (a), $\text{Fe}_3\text{O}_4\text{-CS}$ (b) and $\text{Fe}_3\text{O}_4\text{-CS@MIPs}$ (c) in the 2θ range of 20 to 80° were shown in Fig.3. The (2 2
50 0), (3 1 1), (4 0 0), (4 2 2), (5 1 1), and (4 4 0) planes of Fe_3O_4 were observed at $2\theta=30.14^\circ$, 35.50° , 43.16° , 53.58° , 57.06° and
51 62.62° for three samples, which were consistent with the data of magnetite in the JCPDS-International Centre for Diffraction Data
52 (JCPDS Card: 19-629) file. The results explained that the resultant particles had the same spinel structure as naked Fe_3O_4 and also
53 indicated that the coating polymerization procedure did not result in a crystalline change in Fe_3O_4 . The slight differences in the
54
55
56
57
58
59
60

1 broad nature of the diffraction bands for the three samples were reflected by the different particle sizes; in addition, a broader
2 peak width meant a thicker coating.
3
4

5 The surface morphology of the Fe₃O₄-CS@MIPs was examined by SEM. In Fig.4b, the size of the Fe₃O₄-CS@MIPs, which had
6 a relatively narrow size distribution, was around 34 nm in diameter. Fig.4a showed that there was a porous structure on the
7 surface of the polymer, which was a benefit for increasing the adsorption capacity and improving the mass transfer rate of
8 rebinding and releasing the analyte molecules.
9
10

11 The magnetic properties of the prepared Fe₃O₄, Fe₃O₄-CS and Fe₃O₄-CS@MIPs were studied by VSM at room temperature,
12 and the magnetic hysteresis loops of the three samples were shown in Fig.5. It is obviously seen that there is symmetry about
13 the origin and both the coercivity as well as the resonance were zero. The saturation magnetization values were 69.94, 20.84,
14 and 3.91 emu g⁻¹ with a decreasing tendency. These results manifested the superparamagnetic property of the synthetic MMIPs
15 with a non-magnetic polymer layer coating on the surface of Fe₃O₄-CS. Meanwhile the inset in Fig.5 showed that Fe₃O₄-CS@MIPs
16 were separated from the solution by an external magnetic field in a short 5min, which were beneficial for environmental sample
17 analysis.
18
19
20
21
22
23
24
25
26

27 The TGA analysis of Fe₃O₄, Fe₃O₄-CS and Fe₃O₄-CS@MIPs were shown in Fig.6. For Fe₃O₄, the curve (Fig.6(a)) illustrated that
28 the weight loss was approximately 6% in the temperature range of 30-500 °C due to the loss of residual water in the sample. On
29 the other hand, Fe₃O₄-CS (Fig.6 (b)) and Fe₃O₄-CS@MIPs (Fig.6 (c)) had a rapid weight loss rate between 240-400 °C, which might
30 be due to the loss of the organic polymers on the surface of Fe₃O₄. According to the weight loss percentages in the TGA curves
31 (Fig.6 (b) and Fig.6 (c)), the amounts of CS and imprinted polymer were estimated to be approximately 46.8% and 74.4%
32 respectively, which were higher than the other previous studies contributed by the active Fe₃O₄-CS core.
33
34
35
36
37
38

39 Hence, all of the characterization results fully demonstrated that there was a stable imprinted polymer layer bonded on the
40 surface of the superparamagnetic particles, which was suitable for use in further extraction experiments.
41
42

43 **3.3 Binding properties of Fe₃O₄-CS@MIPs**

44 **3.3.1 Adsorption isotherms**

45 To investigate the binding performances of Fe₃O₄-CS@MIPs and Fe₃O₄-CS@NIPs, the binding experiments were carried out
46 in an aqueous solution instead of in other solvents because MIPs would be applied in water samples. The corresponding
47 adsorption isotherms were shown in Fig.7. The resulting data showed that with an increase in the initial concentrations of SMZ
48 and SMX, the equilibrium adsorption capacity (Q_e) of the MIPs and NIPs for template molecules increased, and the Q_e reached a
49 maximum value when the initial concentration was approximately 240 μg mL⁻¹. The maximum capacities ($Q_{max(SMX)}=4.32$ mg g⁻¹;
50 $Q_{max(SMZ)}=4.13$ mg g⁻¹) of the MIPs were 3.48 and 3.20 times those of the NIPs, respectively, indicating that the surface of the
51
52
53
54
55
56
57
58
59
60

1 Fe₃O₄-CS@MIPs had more cavities with specific adsorption properties and a high affinity for enriching trace SMZ and SMX
 2 compared with the NIPs.
 3
 4

5 Additionally, the common Langmuir and Freundlich isotherm models were used to analyse the adsorption data and are
 6 represented as follows:
 7

$$8 \quad C_e/Q_e = C_e/Q_{max} + 1/kQ_{max}$$

$$9 \quad \ln Q_e = \ln C_e/n + \ln Q_{max}$$

10 where Q_e is the equilibrium adsorption capacity (mg g⁻¹), C_e is the equilibrium adsorption concentration of SMZ or SMX (mg L⁻¹),
 11 Q_{max} is the maximum adsorption capacity (mg g⁻¹), k is the Langmuir adsorption equilibrium constant and n is the Freundlich
 12 adsorption index.
 13
 14
 15
 16
 17
 18
 19

20 The final isotherm parameters shown in Table 2 suggested that the Langmuir isotherm model was more applicable to
 21 estimate the affinity distributions than the Freundlich model according to the correlation coefficients (R^2). From the slope and
 22 intercept of the straight line obtained, the values of K_d and Q_{max} were $K_{d(smz)}=38.11 \text{ mg L}^{-1}$, $K_{d(smz)}=60.23 \text{ mg L}^{-1}$, $Q_{max(smz)}=4.52 \text{ mg}$
 23 g^{-1} , and $Q_{max(smz)}=4.59 \text{ mg g}^{-1}$, respectively. This result was contrary to that of our previous studies [35]. It may be that, in addition
 24 to the interaction between the functional monomers and SAs, the amino groups of Fe₃O₄-CS@MIPs could form hydrogen bonds
 25 with the sulfonyl groups of SAs, which reduced the heterogeneity of the MIPs and improved imprinted adsorption cavities with a
 26 fixed size, a fixed shape and binding sites. It also manifested that the monolayer molecules adsorbed and a homogeneous
 27 distribution of specific cavities existed on the surface of the MIPs.
 28
 29
 30
 31
 32
 33
 34
 35
 36
 37
 38

39 **3.3.2 Adsorption kinetics**

40 The kinetics of adsorption is important to control the process efficiency in practical sample analysis. As shown in Fig.8, the
 41 adsorption capacity reached a plateau after increasing rapidly at approximately 9 min. It may be that the thin imprinted layer
 42 containing the specifically recognized cavities on the surface of Fe₃O₄-CS was in favour of the efficient extraction of the template
 43 molecules and enhanced the mass transfer speed of the target molecules. The benefits of the surface molecular imprinting
 44 technology were particularly demonstrated. Furthermore, pseudo-first-order and pseudo-second-order kinetic models were
 45 applied to investigate the binding process. The equations of the models are as follows:
 46
 47
 48
 49
 50
 51
 52
 53
 54
 55

$$56 \quad \ln(Q_e - Q_t) = \ln Q_e - k_1 t$$

$$t/Q_t = t/Q_e + 1/k_2Q_e^2$$

where Q_t and Q_e represent the adsorption capacities (mg g^{-1}) of the template molecules at a certain time t (min) and adsorption equilibrium and k_1 (min^{-1}) and k_2 ($\text{g mg}^{-1} \text{min}^{-1}$) are the rate constants of the pseudo-first-order and pseudo-second-order models, which can be calculated from the plot of $\ln(Q_e - Q_t)$ versus t and t/Q_t versus t , respectively.

The adsorption rate constants and linear regression values from the two rate equations were summarized in Table 3. According to the correlation coefficient (R^2 values above 0.99) and Q_e (experimental and calculated values), the pseudo-second-order model had a better fit than the pseudo-first-order model for the adsorption of SMZ and SMX. It was assumed that chemisorption could be the rate-limiting step in the adsorption process for template molecules. Meanwhile based on the pseudo-second-order model, the initial adsorption rates (h , $\text{mg g}^{-1} \text{min}^{-1}$) and half equilibrium time ($t_{1/2}$, min) were also calculated as follows and were listed in Table 3.

$$H = k_2Q_e^2$$

$$t_{1/2} = 1/k_2Q_e$$

Comparing the values of h and $t_{1/2}$, the adsorption rates of the template molecules onto the MIPs were higher than those onto the NIPs because the binding sites formed by both the functional monomers and Fe_3O_4 -CS provided an unimpeded channel, in which the target analytes could be rapidly captured.

3.3.3 Selective adsorption

In this study, the aim was that the synthesized polymers not only showed rapid separation performance through the magnetic cores but also displayed "group-selectivity" through the mixed templates for the analysis of practical water samples. Therefore four parameters, namely K_d , k , k' and the recovery, of seven SAs, TMP, CED and CTX were used to evaluate the selectivity of MIPs and NIPs. The data were summarized in Table 4 and Table 5. Furthermore the following results were found: (i) the K_d values of the MIPs for SAs were significantly higher than those of the NIPs. However the K_d values of the MIPs and NIPs for TMP, CEX and CTX exhibited relatively small differences. It was indicated that MIPs, with their strong binding sites supported by the proper functional monomers, were favourable for the selective adsorption of SMZ, SMX and their structural analogues. The shapes and sizes of the three-dimensional cavities in the MIPs were more regular and ordered than those in the NIPs. (ii) The k values of the MIPs for SMZ and SMX were the highest, showing that the active sites left by the template molecule showed the

1 best affinity and specific recognition ability toward them in the MIPs. (iii) The k' value is an indicator to express the adsorption
2
3
4 affinity of recognition sites toward the analytes. The k' values were close to 1, indicating that the MIPs had a binding ability that
5
6 was more similar to the adsorbents, which also meant that the MIPs had the better group-selectivity for SAs in this study. The k'
7
8 values of the SAs followed the order SMX<SIX<SMR<SDM<STZ<SDZ and were all similar. It may be that the same hydrogen bond
9
10 could form between the SAs, 2-VPy and the mixture of template molecules improving the distinct size and structure of the
11
12 recognized cavities. (iv) To evaluate the "group-selectivity" of the MIPs in real samples, recovery experiments were conducted in
13
14 bank wastewater spiked with seven SAs and the typical antibiotics TMP, CTX, and CED at three different concentrations (20, 200
15
16 and 1000 ng mL⁻¹). The recoveries of seven SAs ranged from 85.02 to 102.98%, and the recoveries of TMP, CED and CTX were in
17
18 range of 40.12-44.09%, 32.84-35.33% and 23.15-26.19%, respectively, which were significantly smaller than those of the SAs. The
19
20 clear differences in the recoveries between SAs and other analytes (TMP, CED and CTX) also demonstrated that the MIPs not only
21
22 had special recognition for the target compounds but also eliminated disturbance by impurities in the complicated matrix. These
23
24 above results proved that the synthetic Fe₃O₄-CS@MIPs expressed a superior recognition affinity for SAs and could be practically
25
26 applied for use in aquatic samples.
27

28 **3.4 Method validation**

29
30
31 The external standard method was used for the quantitative analysis of seven SAs in water samples, and calibration curves
32
33 were obtained by plotting the relationship between the peak area and the concentrations of the seven SAs ranging from 10.0 ng
34
35 mL⁻¹ to 2000.0 ng mL⁻¹. The method exhibited a good linear relationship as the correlation coefficients (R^2) of the determination
36
37 curves were greater than 0.999 as shown in Table 6. The LOD in the water samples was defined using the lowest concentration
38
39 producing a signal-to-noise ratio (S/N) of 3 in the range of 5.46-12.13 ng L⁻¹. Furthermore the overall recoveries of seven SAs in
40
41 Table 5 with relative standard deviations (RSD) lower than 6.47%, which conformed to the requirements (80-110%) of the
42
43 Commission Decision 2002/657/EC. As was shown in Table 6, the EF values were estimated by the ratio of SAs concentration of
44
45 post-extraction and pre-extraction procedure in the aqueous sample in the range of 431.52-492.80.
46

47 **3.5 Analysis of practical water samples**

48
49 To verify the applicability of the MMI-DSPE coupled with HPLC method, five water samples were collected and analyzed. SAs
50
51 at detectable levels were not found in drinking water, Laodong Lake water and Nenjiang River water. However, SMX was found in
52
53 wastewater samples taken from the Qiqihar sewage treatment plant. The concentrations of SMX in the influent and effluent
54
55 sewage samples were 112 and 64 ng L⁻¹, respectively. The results indicated that a certain amount of SMX was disposed of
56
57 through wastewater treatment, but it cannot be completely removed. Furthermore, the same wastewater samples (the effluent
58
59
60

samples) were pretreated by MMI-DSPE and C₁₈-SPE, respectively, and HPLC chromatograms were shown in Fig.9, which indicated that MMIPs were more effective to eliminate any matrix interference than C₁₈ in the pre-concentration procedure. Therefore, the proposed method was suitable for the separation and determination of multiple SAs in various water samples.

4 Conclusions

This work has provided a general surface-imprinted method to synthesize core-shell magnetic MIPs using active Fe₃O₄-CS as supporter. Through investigating the adsorption properties of the MIPs, the prepared particles not only exhibited excellent recognition and selection for the imprinted molecules and their analogues but also rapidly reached adsorption equilibrium and easily separated from the analysed matrix. Furthermore the analysed method of MMI-DSPE coupled with HPLC was established and successfully applied for pre-concentrating SAs from some water samples. The good recoveries and enrichment factors also suggested that Fe₃O₄-CS@MIPs is one of the most proposing pre-concentration materials and can be applied in various fields, including environmental pollutants, biochemical separation and pharmaceutical analysis.

Inserting Tables

Tab. 1 Preparation and evaluation of Fe₃O₄-CS@MIPs and Fe₃O₄-CS@NIPs

Polymer	Crosslinker	Mol ratio	$Q_{max}(\text{mg g}^{-1})$		$K_d(\text{mL g}^{-1})$		k		$LF(\%)$	
			SMZ	SMX	SMZ	SMX	SMZ	SMX	SMZ	SMX
MIP1	DVB	1:4:20	3.26	3.64	13.77	15.40	3.02	2.96	—	—
MIP2	EDMA	1:4:20	2.96	3.01	12.48	12.70	2.73	2.44	—	—
MIP3	TRIM	1:4:20	4.13*	4.32*	17.50	18.28	3.83	3.52	4.69	5.11
MIP4	TRIM	1:4:14	1.62*	1.87*	6.79	7.85	1.48	1.51	9.24	13.26
MIP5	TRIM	1:4:16	2.02*	2.44*	8.48	10.27	1.85	1.97	10.11	9.42
MIP6	TRIM	1:4:24	2.99*	3.47*	12.61	14.67	2.76	2.82	4.17	4.69
NIP	TRIM	1:4:20	1.29	1.24	4.56	5.19	—	—	—	—

*the average value of six binding/regeneration cycles experiments

Tab. 2 Langmuir and Freundlich isotherm parameters for adsorption of SMX and SMZ

Adsorption isotherms	Constants	Fe ₃ O ₄ -CS@MIPs-MIP3	
		SMZ	SMX
Langmuir	R^2	0.990	0.995
	$Q_e(\text{mg g}^{-1})$	4.52	4.59
	k	0.038	0.060
Freundlich	R^2	0.886	0.841
	$Q_e(\text{mg g}^{-1})$	1.582	1.739
	n	0.143	0.214

Tab. 3 Pseudo-first-order and Pseudo-second-order parameters for adsorption of SMX and SMZ

Adsorption kinetics	Constants	Fe ₃ O ₄ -CS@MIPs-MIP3		Fe ₃ O ₄ -CS@NIPs	
		SMZ	SMX	SMZ	SMX
Pseudo-first-order	R^2	0.959	0.933	0.914	0.982
	Q_e (mg g ⁻¹)	6.061	6.211	2.052	1.017
	k_1 (min ⁻¹)	0.007	0.008	0.001	0.006
Pseudo-second-order	R^2	0.991	0.995	0.956	0.996
	Q_e (mg g ⁻¹)	4.847	5.078	1.23	1.29
	k_2 (g mg ⁻¹ min ⁻¹)	0.998	1.197	0.017	0.015
	h (mg g ⁻¹ min ⁻¹)	38.630	41.280	36.810	32.22
	$t_{1/2}$ (min)	0.021	0.019	0.135	0.135

Tab.4 Selective adsorption evaluation of seven SAs, TMP, CED and CTX on Fe₃O₄-CS@MIPs-MIP3 and Fe₃O₄-CS@NIPs

Analytes	K_D (mL g ⁻¹)		k	k'
	Fe ₃ O ₄ -CS@MIPs-MIP3	Fe ₃ O ₄ -CS@NIPs		
SMZ	17.50	4.56	3.83	-
SMX	18.28	5.19	3.52	1.09
SIX	16.84	5.01	3.36	1.14
SMR	15.92	4.79	3.32	1.15
STZ	13.17	4.47	2.94	1.30
SDM	14.26	4.72	3.02	1.27
SDZ	13.99	4.97	2.81	1.36
TMP	7.98	5.74	1.39	2.75
CED	4.44	4.53	0.98	3.91
CTX	4.89	4.04	1.21	3.16

Tab.5 Recoveries of seven SAs, TMP, CED and CTX spiked at three concentration levels

Analytes	20 ng L ⁻¹		200 ng L ⁻¹		1000 ng L ⁻¹	
	Recovery (%)	RSD (%)	Recovery (%)	RSD (%)	Recovery (%)	RSD (%)
SMZ	90.16	3.10	96.71	5.45	95.99	2.92
SMX	94.39	2.77	98.31	3.43	102.98	3.18
SIX	86.91	6.45	92.22	6.47	91.23	4.86
SMR	88.09	3.91	89.37	3.76	89.07	2.42
STZ	89.14	3.91	88.61	4.54	90.31	3.66
SDM	93.99	4.44	89.89	3.19	85.89	3.56
SDZ	87.17	5.28	86.72	4.19	85.02	2.49
TMP	40.12	3.11	42.96	4.19	44.09	3.45
CED	32.84	2.78	35.33	3.09	34.09	2.65
CTX	23.15	4.23	26.19	5.11	24.78	1.99

Tab.6 Calibration curve, LOD and EF of seven SAs

Analytes	Calibration curve	R^2	LOD (ng L ⁻¹)	EF
SMZ	$y^a = 399.6x^b - 0.263$	0.9996	9.71	471.43
SMX	$y = 567.1x + 0.214$	0.9994	12.13	492.80
SIX	$y = 572.9x + 0.051$	0.9995	6.68	450.60

SMR	$y = 409.9x - 0.070$	0.9991	5.93	444.22
STZ	$y = 310.9x - 0.177$	0.9991	7.67	446.77
SDM	$y = 529.4x - 0.318$	0.9993	10.17	449.62
SDZ	$y = 336.1x - 0.462$	0.9994	5.46	431.52

^a The peak area of HPLC

^b The concentration of analytes (ng mL⁻¹)

Reference

a State Key Laboratory of Urban Water Resource and Environment, School of Municipal and Environmental Engineering, Harbin Institute of Technology, Harbin, China. Huanghe Road 73, Nangang District, Harbin, E-mail: pwang73@hit.edu.cn; Fax: +86 86283557; Tel: +86-0451-86283557

b Key Laboratory of Applied Chemistry, School of Chemistry and Chemical Engineering, Qiqihar University, Qiqihar, China. Wenghua Street 42, Jianhua District, Qiqihar, E-mail: slq202@163.com; Fax: +86 2738214; Tel: +86-0452-2738214

- [1] D. A. Dibbern Jr, A. Montanaro, *Ann. Allergy, Asthma, Immunol.*, 2008, 100, 91-101
- [2] B. Schnyder, W. J. Pichler, *J. Allergy Clin. Immunol.*, 2013, 131, 256-257
- [3] Glenn D. Considine, *Van Nostrand's encyclopedia of chemistry, Sulfonamide Drugs*, London, 2005
- [4] W. Baran, E. Adamek, J. Ziemiańska, A. Sobczak, *J. Hazard. Mater.*, 2011, 196, 1
- [5] P. Gao, D. Mao, Y. Luo, L. Wang, B. Xu, L. Xu, *Water Research*, 2012, 46, 2355
- [6] J. H. Su, C. Chen, C. Young, W. Chao, M. Li, Y. Liu, C. Lin, C. Ying, *J. Hazard. Mater.*, 2014, 277, 34
- [7] A. Karci, I.A. Balcioğlu, *Sci. Total Environ.*, 2009, 407, 4652
- [8] H. Kim, Y. Hong, J. Park, V. K. Sharma, S. Cho, *Chemosphere*, 2013, 91, 888
- [9] Z. Lu, G. Na, H. Gao, L. Wang, C. Bao, Z. Yao, *Sci. Total Environ.*, 2015, 527-528, 429
- [10] A. Białk-Bielińska, J. Kumirska, R. Palavinskas, P. Stepnowski, *Talanta*, 2009, 80, 947
- [11] J. Raich-Montiu, J. Folch, R. Compañó, M. Granados, M.D. Prat, *J. Chromatogr. A*, 2007, 1172, 186
- [12] V. K. Balakrishnan, K. A. Terry, J. Toito, *J. Chromatogr. A*, 2006, 1131, 1
- [13] A. Jia, J. Hu, X. Wu, H. Peng, S. Wu, Z. Dong, *Environ. Toxicol. Chem.*, 2011, 30, 1252-1260
- [14] S.G. Dmitrienko, E. V. Kochuk, V. V. Apyari, V.V. Tolmacheva, Y.A. Zolotov, *Anal. Chim. Acta*, 2014, 850, 6
- [15] A. Martín-Esteban, *TrAC, Trends Anal. Chem.*, 2013, 45, 169
- [16] J. Tan, Z.T. Jiang, R. Li, X.P. Yan, *TrAC, Trends Anal. Chem.*, 2012, 39, 207
- [17] J.A. García-Calzón, M.E. Díaz-García, *Sens. Actuators, B*, 2007, 123, 1180
- [18] J. O. Mahony, K. Nolan, M. R. Smyth and, B. Mizaikoff, *Cheminform*, 2005, 36,
- [19] F. Tan, D. Sun, J. Gao, Q. Zhao, X. Wang, F. Teng, X. Quan, J. Chen, *J. Hazard. Mater.*, 2013, 244–245, 750
- [20] M. Doué, E. Bichon, G. Dervilly-Pinel, Valérie Pichon, F. Chapuis-Hugon, E. Lesellier, C. West, F. Monteau, B.L. Bizec, *J. Chromatogr. A*, 2012, 1270, 51
- [21] Núria Gilart, R.M. Marcé, Núria Fontanals, F. Borrull, *Talanta*, 2013, 110, 196
- [22] Z. Long, Y. Lu, M. Zhang, H. Qiu, *J. Sep. Sci.*, 2014, 37, 2764

- 1 [23] X. Su, X. Li, J. Li, M. Liu, F. Lei, X. Tan, P. Li, W. L., *Food Chem.*, 2015, 171, 292
- 2
- 3 [24] J. Yang, Z. Wang, T. Zhou, X. Song, Q. Liu, Y. Zhang, L. He, *J. Chromatogr. B*, 2015, 990, 39
- 4
- 5 [25] B.B. Prasad, A. Srivastava, A. Prasad, M.P. Tiwari, *Colloids Surf. B*, 2014, 113, 69
- 6
- 7 [26] B. Li, Y. Zhou, W. Wu, M. Liu, S. Mei, Y. Zhou, T. Jing, *Biosens. Bioelectron.*, 2015, 67, 121
- 8
- 9 [27] E. Turiel, A. Martín-Esteban, J. Tadeo, *J. Chromatogr. A*, 2007, 1172 (2), 97
- 10
- 11 [28] L.Y. Guo, X. Jiang, C.L. Yang, H. Zhang, *Anal. Bioanal. Chem.*, 2008, 391, 2291
- 12
- 13 [29] R. Gao, J. Zhang, X.W. He, L.X. Chen, Y.K. Zhang, *Anal. Bioanal. Chem.*, 2010, 398, 451
- 14
- 15 [30] W. Liu, X. Liu, Y. Yang, Y. Zhang, B. Xu, *Fuel*, 2014, 117, 184
- 16
- 17
- 18 [31] Y. Duan, C. Dai, Y. Zhang, L. Chen, *Anal. Chim. Acta*, 2013, 758, 93
- 19
- 20 [32] C. Dai, J. Zhang, Y. Zhang, X. Zhou, Y. Duan, S. Liu, *Chem. Eng. J.*, 2012, 211–212, 302
- 21
- 22
- 23 [33] C. Huang, Z. Tu, X. Shen, *J. Hazard. Mater.*, 2013, 248–249, 379
- 24
- 25 [34] T. Jing, Y. Wang, Q. Dai, H. Xia, J. Niu, Q. Hao, S. Mei, Y. Zhou, *Biosens. Bioelectron.*, 2010, 25, 2218
- 26
- 27
- 28 [35] S. Qin, L. Su, P. Wang, S. Deng, *J. Appl. Polym. Sci.*, 2015, 132, 41491
- 29
- 30 [36] L. Yan, K. Yang, R. Shan, T. Yan, J. Wei, S. Yu, H. Yu, B. Du, *J. Colloid Sci.*, 2015, 448, 508
- 31
- 32 [37] M. Stefan, C. Leostean, O. Pana, M. Soran, R. Suciuc, E. Gautron, O. Chauvet, *Appl. Surf. Sci.*, 2014, 288, 180
- 33
- 34 [38] L. Li, K. Sun, L. Fan, W. Hong, Z. Xu, L. Liu, *Mater. Lett.*, 2014, 126, 197
- 35
- 36 [39] Y. Yao, S. Miao, S. Yu, L. Ma, H. Sun, S. Wang, *Colloid Interface Sci.*, 2012, 379, 20
- 37
- 38 [40] Y. Zhao, Y. Yeh, R. Liu, J. You, F. Qu, *Solid State Sci.*, 2015, 45, 9
- 39
- 40 [41] L. Chen, X. Zhang, L. Sun, Y. Xu, Q. Zeng, H. Wang, H. Xu, A. Yu, H. Zhang, L. Ding, *J. Agric. Food Chem.*, 2009, 57, 10073
- 41
- 42 [42] X. Kong, R. Gao, X. He, L. Chena, Y. Zhang, *J. Chromatogr. A.*, 2012, 1245, 8
- 43
- 44 [43] X. Mao, H. Sun, X.W. He, L.X. Chen, Y.K. Zhanga, *Anal. Methods*, 2015, 7, 4708
- 45
- 46
- 47 [44] L. Liu, L. Xiao, H. Zhu, *Chem. Phys. Lett.*, 2012, 539–540, 112
- 48
- 49 [45] W. Cheng, Z. Liu, Y. Wang, *Talanta*, 2013, 116, 396
- 50
- 51 [46] L. Li, X. He, L. Chen, Yi Zhang, *Chem. - Asian J.*, 2009, 4, 286
- 52
- 53 [47] X. Chen, Z. Zhang, X. Yang, Y. Liu, J. Li, M. Peng, S. Yao, *J. Sep. Sci.*, 2012, 35, 2414
- 54
- 55 [48] W. Guo, W. Hu, J. Pan, H. Zhou, W. Guan, X. Wang, J. Dai, L. Xu, *Chem. Eng. J.*, 2011, 171, 603
- 56
- 57 [49] S. Qin, S. Deng, L. Su, P. Wang, *Anal. Methods.*, 2012, 4, 4278
- 58
- 59
- 60

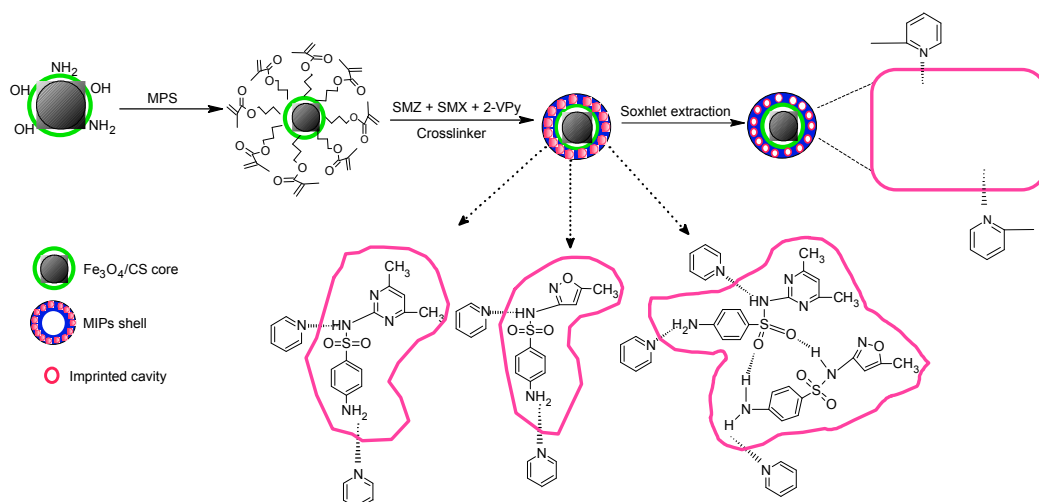


Fig.1. Synthesis route of surface-imprinted core-shell magnetic beads and effect protocol for mixed-templates and 2-Vpy

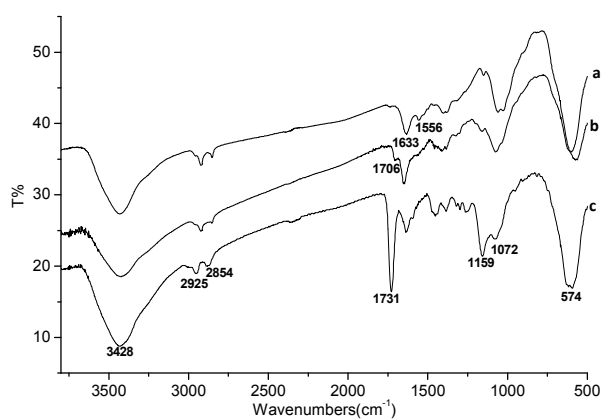


Fig.2. FT-IR spectra of $\text{Fe}_3\text{O}_4\text{-CS}$ (a), vinyl-modified $\text{Fe}_3\text{O}_4\text{-CS}$ (b) and $\text{Fe}_3\text{O}_4\text{-CS@MIPs}$ (c)

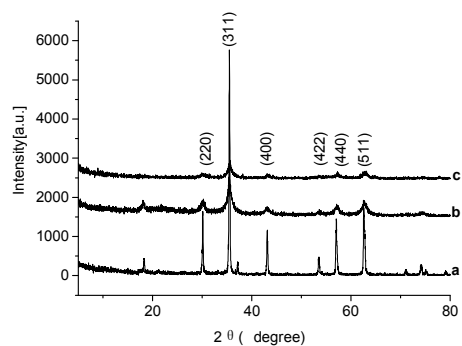


Fig.3. XRD patterns of Fe_3O_4 (a), $\text{Fe}_3\text{O}_4\text{-CS}$ (b) and $\text{Fe}_3\text{O}_4\text{-CS@MIPs}$ (c)

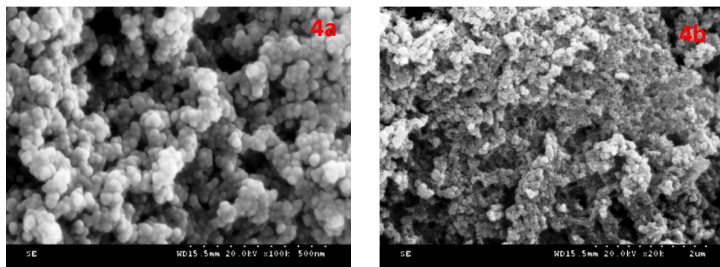


Fig. 4. SEM images of Fe₃O₄-CS@MIPs with different magnification (4a-100K, 4b-20K)

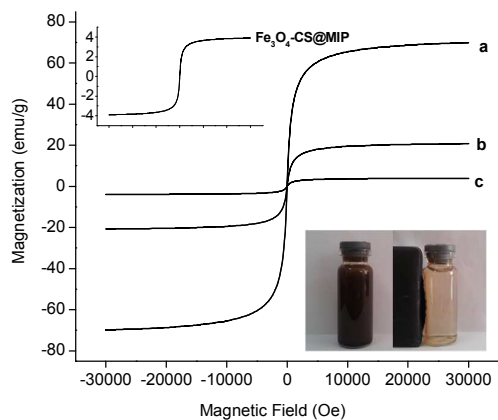


Fig. 5. Hysteresis loops of Fe₃O₄ (a), Fe₃O₄-CS (b) and Fe₃O₄-CS@MIPs (c) and the insert (bottom right) shows the separation and re-dispersion process of an aqueous solution of Fe₃O₄-CS@MIPs in the absence (left) and presence (right) of an external magnetic field.

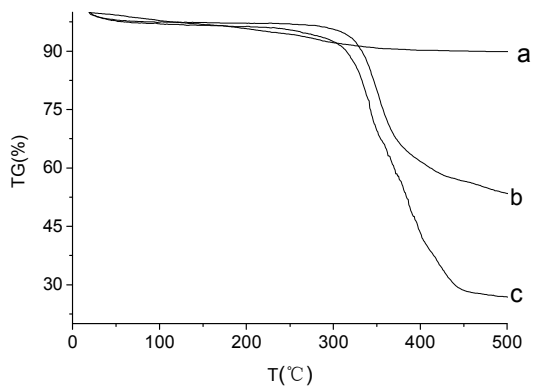


Fig. 6. TGA curves of Fe₃O₄ (a), Fe₃O₄-CS (b) and Fe₃O₄-CS@MIPs (c)

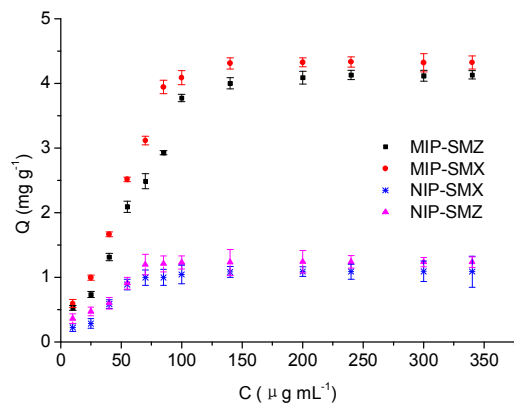


Fig.7. Adsorption equilibrium isotherm of the MIPs and NIPs for SMX and SMZ

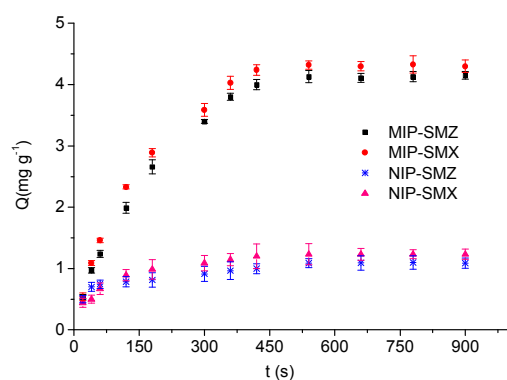


Fig.8. Adsorption kinetic curves of the MIPs and NIPs for SMX and SMZ

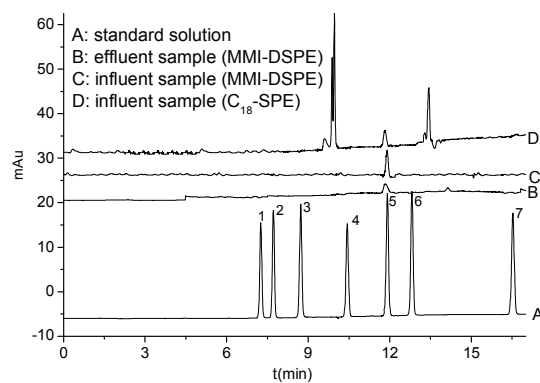
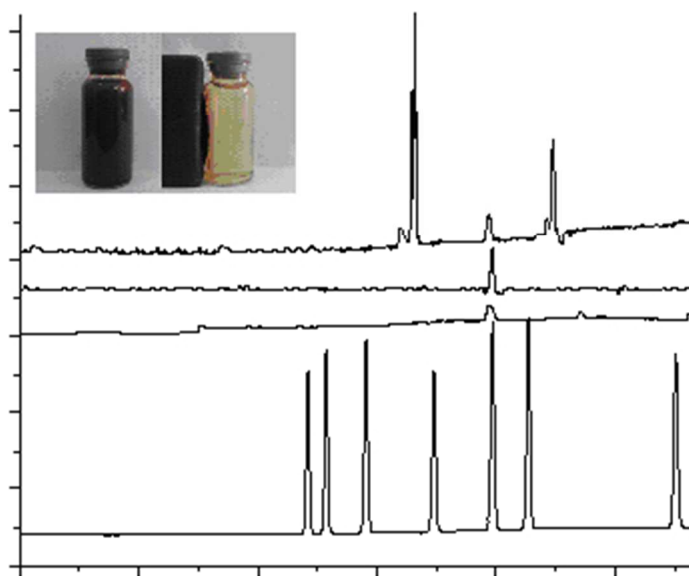


Fig.9. The chromatographic profiles at 270nm from the analysis of wastewater samples through different SPE methods

1:STZ;2:SDZ;3:SMR;4:SMZ;5:SMX;6:SIX;7:SDM

1
2
3
4
5
6
7
8
9
10
11
12
13
14
15
16
17
18
19
20
21
22
23
24
25
26
27
28
29
30
31
32
33
34
35
36
37
38
39
40
41
42
43
44
45
46
47
48
49
50
51
52
53
54
55
56
57
58
59
60



Highly selective MIPs-MDSPE/HPLC method for fast extraction and determination of seven SAs

105x94mm (96 x 96 DPI)